29th EPS Conference on Plasma Phys. and Contr. Fusion Montreux, 17-21 June 2002 ECA Vol. **26B**, P-2.096 (2002)

Linear Wave Model of the DED Field*

Christian G. Eherer[1], Martin F. Heyn[1], Sergei V. Kasilov[2], Winfried Kernbichler[1]

[1] *Institut für Theoretische Physik, Technische Universität Graz, Petersgasse 16, A–8010 Graz, Austria*

[2] *Institute of Plasma Physics, National Science Center "Kharkov Institute of Physics and Technology", Ul. Akademicheskaya 1, 61108 Kharkov, Ukraine*

Introduction

In the concept of DED, external perturbation coils create at the edge a rotating helical field whose frequency can be changed from dc to a few kilohertz depending on the operational regime. For medium to high frequencies the plasma response near the resonant surface where the confining background magnetic field is parallel to the currents inside the DED field coils becomes important and one expects reasonably well established ergodic transport which smears out the heat load [1]. In the present contribution, the local wave dispersion is studied within different approximations of the two fluid description of a plasma. This leads to a model which takes into account parallel electron pressure, ion pressure as well as compressional and gyro ion viscosities. On this basis, the linear wave problem of field penetration for TEXTOR-like parameters is solved.

Basic Equations

Because of the low frequencies involved in the problem, the compressional as well as the gyro viscosity of the ions is taken into account in the electron-ion fluid model. The equations to be solved are Maxwell equations for the fields and the Braginskii equation set [2] for the particles,

$$\nabla \times \mathbf{E} = -\frac{1}{c}\frac{\partial \mathbf{B}}{\partial t}, \qquad \nabla \times \mathbf{B} = \frac{4\pi}{c}\sum_\alpha e_\alpha n_\alpha \mathbf{V}_\alpha + \frac{1}{c}\frac{\partial \mathbf{E}}{\partial t}. \tag{1}$$

$$\frac{\partial n_\alpha}{\partial t} + \nabla \cdot (n_\alpha \mathbf{V}_\alpha) = 0, \tag{2}$$

$$m_\alpha n_\alpha \left(\frac{\partial}{\partial t} + \mathbf{V}_\alpha \cdot \nabla\right)\mathbf{V}_\alpha = -\nabla (n_\alpha T_\alpha) - \nabla \cdot \mathbf{\Pi}_\alpha - e_\alpha n_\alpha \left(\mathbf{E} + \frac{1}{c}\mathbf{V}_\alpha \times \mathbf{B}\right) + \mathbf{R}_\alpha, \tag{3}$$

$$\frac{3}{2} n_\alpha \left(\frac{\partial}{\partial t} + \mathbf{V}_\alpha \cdot \nabla\right) T_\alpha + n_\alpha T_\alpha \nabla \cdot \mathbf{V}_\alpha = -\nabla \cdot \mathbf{q}_\alpha, \tag{4}$$

$$\mathbf{R}_\alpha = \pm 0.51 \frac{m_e n_e}{\tau_e}\, \mathbf{h} \cdot (\mathbf{V}_e - \mathbf{V}_i)\,, \tag{5}$$

$$\mathbf{q}_e = -3.16 \frac{n_e T_e \tau_e}{m_e}\, \mathbf{hh} \cdot \nabla T_e, \qquad \mathbf{q}_i = -3.9 \frac{n_i T_i \tau_i}{m_i}\, \mathbf{hh} \cdot \nabla T_i, \tag{6}$$

$$\mathbf{\Pi}_\alpha = -\eta_0 \frac{3}{2}\left(\mathbf{hh} - \frac{1}{3}\mathbf{I}\right)\mathbf{h} \cdot \mathbf{W} \cdot \mathbf{h}$$

$$+ \eta_3 \frac{1}{2}(\mathbf{hh} - \mathbf{I}) \cdot (\mathbf{W} \times \mathbf{h} + \mathbf{h} \times \mathbf{W}) + \eta_4 \mathbf{hh} \cdot (\mathbf{h} \times \mathbf{W} + \mathbf{W} \times \mathbf{h})\,, \tag{7}$$

$$W_{ij} = \partial_i V_j + \partial_j V_i - \frac{2}{3}\delta_{ij} \nabla \cdot \mathbf{V}, \qquad \mathbf{h} = \frac{\mathbf{B}}{B}, \tag{8}$$

*This work has been carried out within the Association EURATOM-ÖAW.

$$\eta_0 = 0.96 n_i T_i \tau_i, \quad \eta_3 = \tfrac{1}{2}\tfrac{n_i T_i}{\omega_i}, \quad \eta_4 = 2\eta_3. \tag{9}$$

For the electrons viscosity is neglected and the pressure force $-\nabla(n_e T_e) - \nabla\cdot\mathbf{\Pi}_e$ is taken to be $-\nabla(n_e T_e)$ (additional mode) and $-\mathbf{hh}\cdot\nabla n_e T_e$, respectively.

The tokamak is modelled as a periodic cylinder and Fourier expansion is done with respect to time, poloidal, and "toroidal" angle. As a result, a set of ordinary differential equations in the radial variable r for the respective Fourier amplitudes is obtained. Independent vectors satisfying the boundary conditions (obtained from the analytic solution of the homogeneous cylinder) at the magnetic axis and at the wall are integrated toward the antenna using repeated orthonormalisation. The conditions at the antenna determine the final linear combination of the solution vectors which are rescaled in a backward run. The antenna coils are modelled as a set of 16 current filaments. These are located at the high field side of TEXTOR.

Results

The wave dispersion is studied for different approximations in order to obtain a model which, on one hand, covers all aspects of physical interest and, on the other hand, does not contain modes whose wavelengths are too small for a reasonable numerical treatment (much less than the ion gyro radius). Figure 1 shows the results for the local wave dispersion as it can be expected for TEXTOR. In the top panel on the left, the results for a model without viscosity but taking into account all components of the electron and ion pressure force are shown. There exist four different wave modes (quartic equation for $k_\perp^2$, $k_\perp^2 = k_r^2 + k_\vartheta^2$, $k_\vartheta^2 = m^2/r^2$; modes of the same type but travelling in opposite directions are counted only once), the fast mode (blue) with the longest wavelength, two modes (green and red) with wavelength of the order of the ion gyro radius (turquoise), and an electron mode (yellow) with wavelength below the electron gyro radius (magenta). The presence of this extremely small scale electron mode will not allow for a solution of the problem with reasonable computing resources. In the right panel, the results are shown when the perpendicular electron pressure force is neglected. The small scale electron mode is absent (a cubic equation for $k_\perp^2$ is obtained) and the model is likely to have all the properties looked for.

The problem arises when reducing the frequency below roughly 1 kHz. The mid panel on the left shows that there is still a mode present (green-red) whose $k_\perp$ values grow like $1/\omega$ and for 100 Hz again a mode with wavelength of the electron gyro radius is observed. However, this $1/\omega$ dependence is removed when taking into account the compressional and the gyro viscosity of the ions. The inclusion of viscosity in the ion momentum equation enhances the number of different modes to four. But now, all four modes are practically independent of the frequency as can be seen in the mid panel on the right(100 Hz) and in the bottom panel on the left (1kHz). The wavelengths of all four modes vary on a reasonable scale for numerical treatment. In the bottom panel on the right, details of the dispersion near the resonant surface at $r = 43.55$ are shown. The spiky behaviour separates small regions of wave evanescence and propagation.

Figure 2 shows the results of the numerical calculation for a TEXTOR-like varying background. The top panel shows the results for the linear perturbations of the magnetic field $|B_\parallel|$ along the background field and the component within the cylindrical surface $|B_\perp|$ perpendicular to the background field (the total normal magnetic field component is $\sqrt{|B_\perp|^2 + |B_r|^2}$). Results are shown without electron background velocity (green) and when taking into account an electron background parallel velocity (blue) such that the

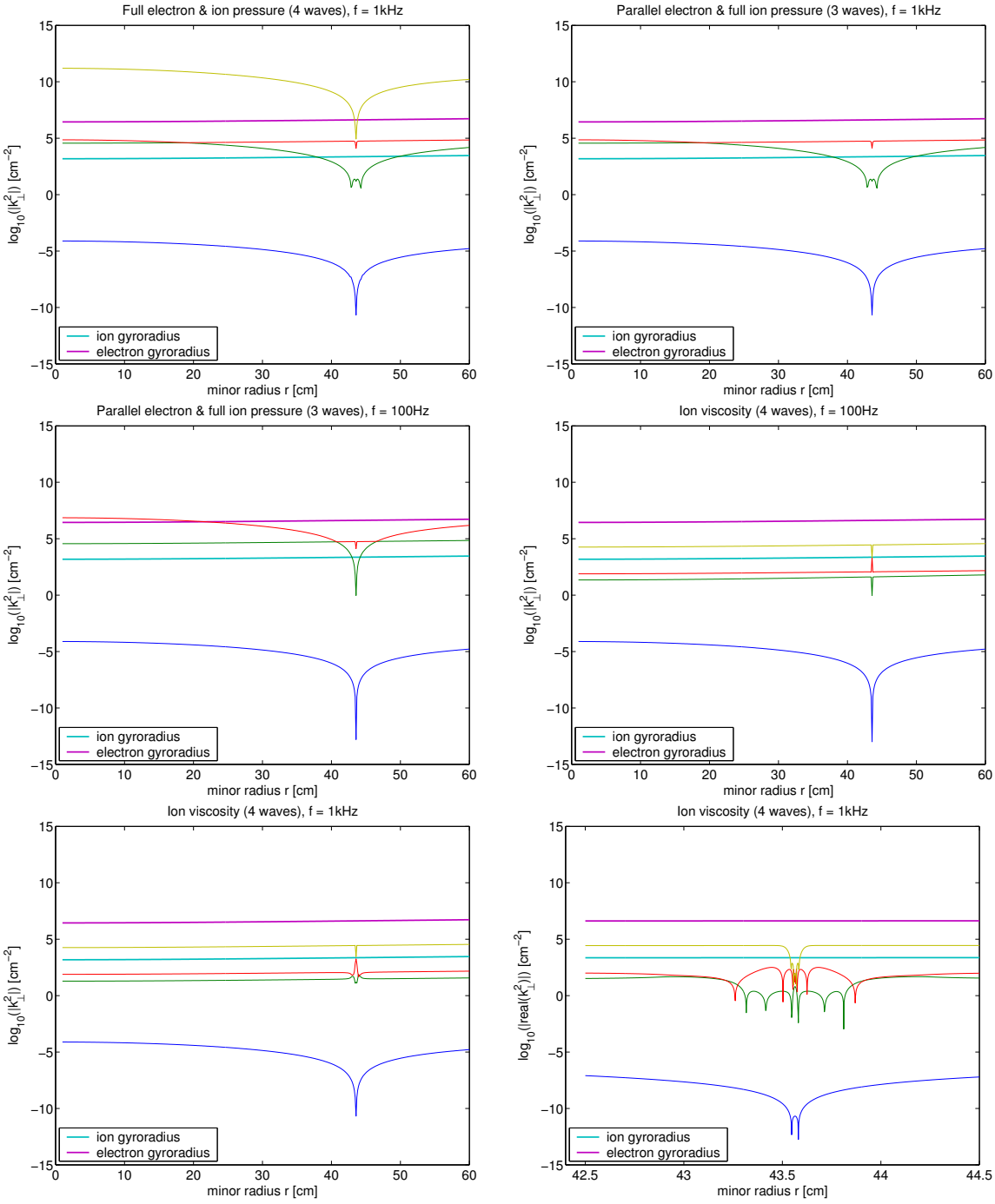

Fig. 1. Solution $k_\perp^2$ of the local dispersion equation as a function of the minor radius r for a safety factor profile with the resonant surface at $q = 3$ ($r = 43.55\,\mathrm{cm}$). Also shown are the corresponding k^2 values of the electron and ion gyro radii.

corresponding current produces the correct safety factor (q-profile). The screening effect of the currents induced near the resonant surface can be observed. The bottom panel shows on the left the behaviour of $|B_r|$ near the resonance and, on the right, the linear (green and blue) and also the time and angle averaged current densities (turquoise and red). The latter current will change the background magnetic field (and, in particular, the resonant surface location) in a quasilinear description of the problem.

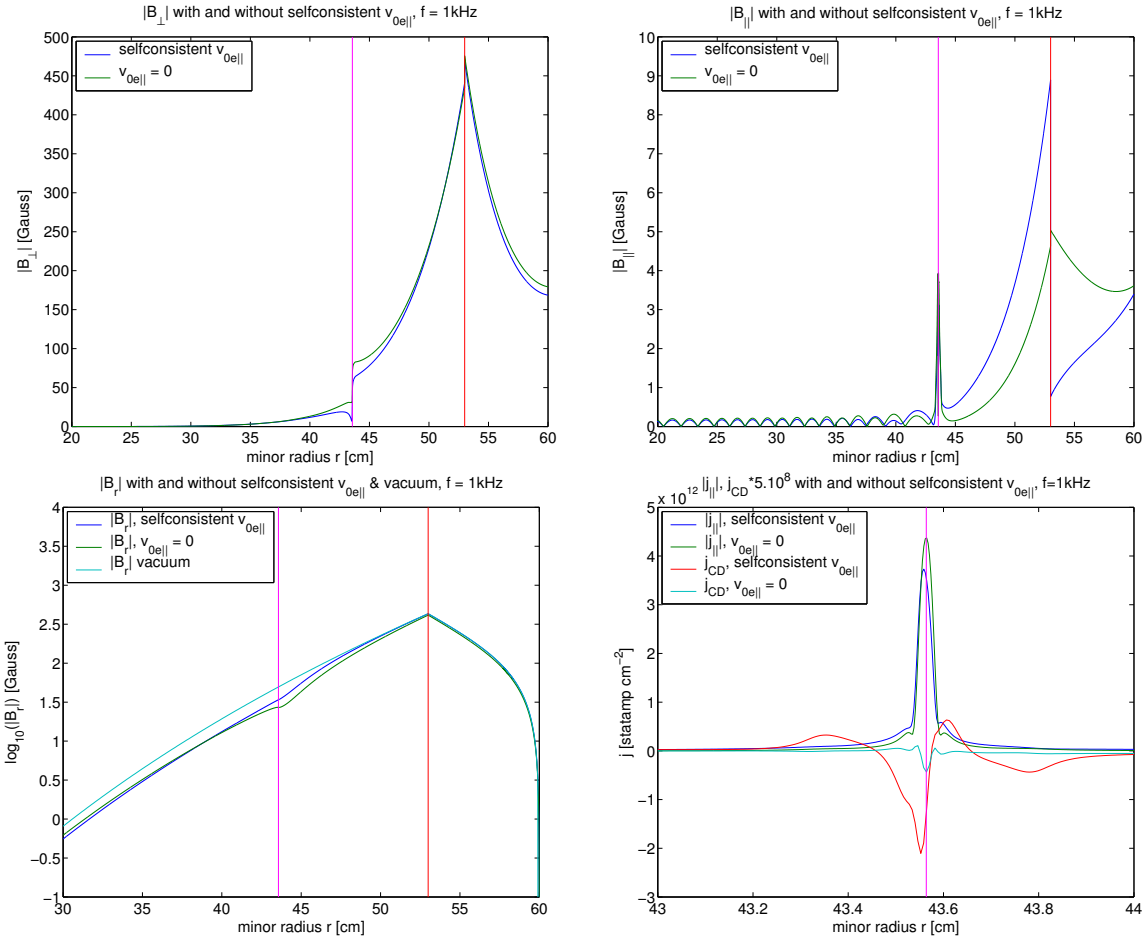

Fig. 2. Results of the numerical integration of the field-particle equations including ion viscosities. The resonant surface has been placed at $r = 43.55\,\mathrm{cm}$. The frequency of the perturbations is 1 kHz.

Conclusions

The results of the linear wave code show that all perturbed quantities such as plasma density, parallel electron velocity stay below their equilibrium values for nominal DED current operation. Therefore, the present linear model is a reasonable approximation. The "slow" selfconsistent evolution of the background plasma parameters (poloidal magnetic field, poloidal and toroidal rotational velocities) will be obtained from the quasilinear model where the quadratic terms (averaged forces, etc.) are evaluated from the results of linear calculations as presented above.

References

[1] Finken, K. H., Eich, T., Abdullaev, S. S., Kaleck, A., Mank, G., Reiser, D., Runov, A., and Tokar', M., Modelling of the Dynamic Ergodic Divertor of TEXTOR-94, *J. Nucl. Materials*, **266–269**, 495–500, 1999.

[2] S.I. Braginskii, in *Reviews of Plasma Physics*, Vol.1, pp. 205-311, 1965.